

# FC-VFI: FAITHFUL AND CONSISTENT VIDEO FRAME INTERPOLATION FOR HIGH-FPS SLOW MOTION VIDEO GENERATION

Ganggui Ding\*    Hao Chen\*    Xiaogang Xu †

\* Zhejiang University † Chinese University of Hong Kong

## ABSTRACT

Large pre-trained video diffusion models excel in video frame interpolation but struggle to generate high fidelity frames due to reliance on intrinsic generative priors, limiting detail preservation from start and end frames. Existing methods often depend on motion control for temporal consistency, yet dense optical flow is error-prone, and sparse points lack structural context. In this paper, we propose FC-VFI for faithful and consistent video frame interpolation, supporting 4× and 8× interpolation, boosting frame rates from 30 FPS to 120 and 240 FPS at 2560 × 1440 resolution while preserving visual fidelity and motion consistency. We introduce a temporal modeling strategy on the latent sequences to inherit fidelity cues from start and end frames and leverage semantic matching lines for structure-aware motion guidance, improving motion consistency. Furthermore, we propose a temporal difference loss to mitigate temporal inconsistencies. Extensive experiments show FC-VFI achieves high performance and structural integrity across diverse scenarios.

*Index Terms*— Computer Vision, Video Frame Interpolation, Video Generation, Diffusion Model, Generative Model

## 1. INTRODUCTION

Video Frame Interpolation (VFI) [1] is a fundamental task in computer vision that aims to synthesize intermediate frames between given start and end frames. It has broad applications, including animation production [2] and slow motion video generation [3].

**Background.** Traditional VFI methods [3, 1] typically rely on motion representations to synthesize intermediate frames, e.g., estimating optical flow between the start and end frames. However, these approaches often struggle in complex scenes where dense motion is difficult to estimate accurately. To address this limitation, diffusion-based methods have recently emerged [4, 5], leveraging generative capabilities to handle such challenging cases. These approaches generally encode the start and end frames into a latent space and use them as conditioning inputs to predict the latent representation of the intermediate frames.

**The challenges of current diffusion-based VFI methods.** However, current diffusion-based VFI methods still exhibit notable weaknesses, e.g., the fidelity issue caused by generative models [6, 7] and the temporal inconsistency of interpolated results [8]. Fidelity issues often manifest as artifacts or structural distortions in the intermediate frames. For instance, a car may appear deformed compared to its shape in the start and end frames, leading to flickering and perceptual inconsistency, as shown in Fig. 2.

Moreover, despite the strong generative priors of diffusion models, the motion in interpolated sequences may still exhibit inaccuracies. To mitigate these issues, some approaches incorporate optical flow or sparse correspondence points to guide motion [7, 4]. However, optical flow estimation can be error-prone in complex scenes [9, 7], potentially degrading interpolation quality, while sparse points are insufficient to capture detailed object structure.

Furthermore, the efficiency of current diffusion-based VFI methods remains a concern. Many approaches generate video frames from the start and end frames independently, and subsequently merging them to produce the final result through bidirectional time-reversal fusion [10, 11, 12]. Some methods even require additional re-noising steps [10, 13], further increasing computational overhead.

**Our model.** In this paper, we propose FC-VFI for faithful and consistent video frame interpolation. Finetuned from a pre-trained large-scale I2V model, our method supports 4× and 8× interpolation at resolutions up to 2560 × 1440, eliminates the need for bidirectional inference, compared to previous diffusion-based methods.

To improve visual fidelity, we propose Temporal Fidelity Modulation Reference (TFMR), a novel temporal modeling strategy. Unlike existing diffusion-based methods that typically perceive conditional latents via channel-wise concatenation [14, 15, 16], TFMR combines the noise of the intermediate frames with the start and end frames along temporal dimension, and perform fidelity modulation on both boundary frames. This design ensures that the intermediate frames consistently reference features from both endpoints throughout the generation process.

To mitigate the near-static behavior between interpolated adjacent frames, we introduce a temporal difference loss that explicitly aligns the predicted motion difference between consecutive frames with that of the ground truth.

To enhance temporal consistency, we introduce a novel conditioning mechanism based on semantic matching lines, which offers greater robustness than optical flow by focusing only on key motion boundaries, and provide richer structural information than sparse points by describing the object shape.

In summary, our contributions are threefold:

- We propose an effective training strategy to fine-tune pre-trained I2V diffusion models into VFI networks, enabling practical interpolation, e.g., from 30 FPS to 120 FPS and 240 FPS for 2560 × 1440 videos.
- We introduce a novel temporal modeling strategy to address fidelity issues in interpolation, alongside a matching lines condition control mechanism and a temporal difference loss to achieve consistent and accurate motion.
- Extensive qualitative and quantitative experiments demonstrate the superiority of our model for 4× and 8× interpolation tasks, highlighting its robust stability and structural consistency, as shown in Fig. 2 and Table 1.

HC and XX are co-corresponding authors.

This work was supported by the “Pioneer” and “Leading Goose” R&D Program of Zhejiang (Grant No. 2025C01011) and the National Natural Science Foundation of China (No. 62576315).

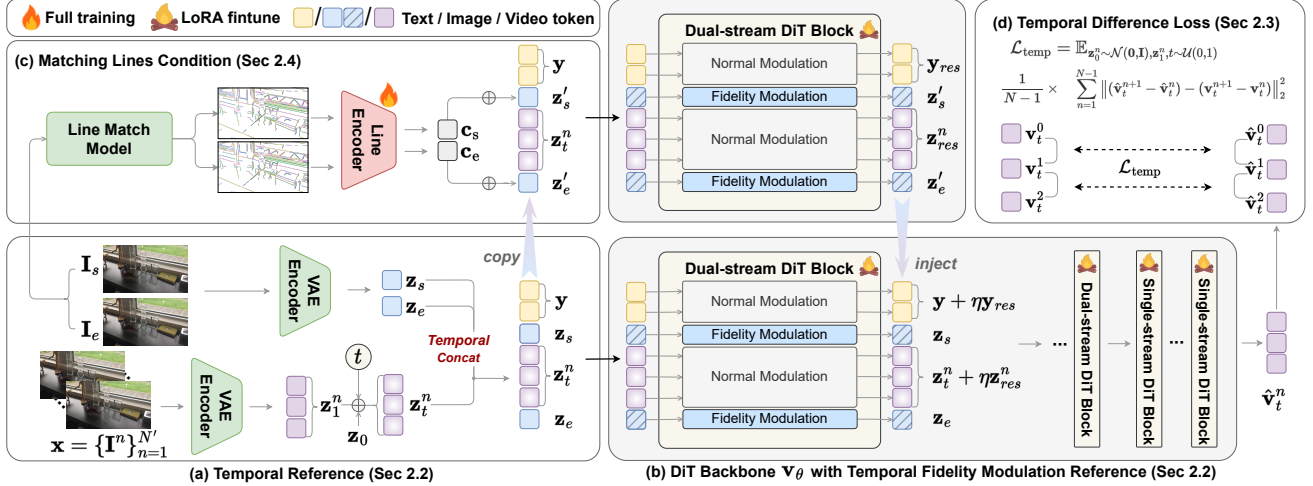


**Fig. 1. Overview of FC-VFI’s training pipeline.** (a) We model temporal references by concatenating the noisy latent  $\mathbf{z}_t^n$  with the start and end image latents  $\mathbf{z}_s$  and  $\mathbf{z}_e$  along the temporal dimension, enabling the denoising process to reference both boundaries. (b) We apply *fidelity modulation* by performing a timestep-dependent modulation  $t^*$  into  $\mathbf{z}_s$  and  $\mathbf{z}_e$ , which enhances reference stability. (c) Semantic matching lines features  $\mathbf{c}_s$  and  $\mathbf{c}_e$  are extracted and encoded from the start frame  $\mathbf{I}_s$  and end frame  $\mathbf{I}_e$ , and are element-wise added to  $\mathbf{z}_s$  and  $\mathbf{z}_e$ , resulting in enhanced latents  $\mathbf{z}'_s$  and  $\mathbf{z}'_e$ . These are then processed via a copied DiT block to produce  $\mathbf{z}^n_{res}$ , which is injected back into the main backbone. (d) The prediction  $\hat{\mathbf{v}}_t^n$  is supervised with a temporal difference loss  $\mathcal{L}_{temp}$ .

## 2. METHOD

### 2.1. Preliminary: Flow Matching Model

Flow Matching (FM) [20] is a generative framework that learns a continuous mapping between Gaussian noise and the target data distribution. Given a video  $\mathbf{x} \in \mathbb{R}^{N' \times 3 \times H' \times W'}$ , it is first encoded by a VAE [21] encoder  $\mathcal{E}$  into a latent  $\mathbf{z}_1 \in \mathbb{R}^{N \times C \times H \times W}$ , where  $C$  is channel dimension,  $N = N'/\lambda_t$ ,  $H = H'/\lambda_s$ , and  $W = W'/\lambda_s$  ( $\lambda_t, \lambda_s$  as temporal and spatial compression ratios of the  $\mathcal{E}$ , respectively). A noisy latent is then obtained as:  $\mathbf{z}_t = (1 - t)\mathbf{z}_1 + t\mathbf{z}_0$ ,  $\mathbf{z}_0 \sim \mathcal{N}(\mathbf{0}, \mathbf{I})$ , where  $t \in [0, 1]$ . The training objective for a I2V model [22, 14] minimizes the discrepancy between the predicted velocity  $\mathbf{v}_\theta$  and the true velocity  $\mathbf{v}_t = \mathbf{z}_0 - \mathbf{z}_1$ :

$$\mathcal{L}_{flow} = \mathbb{E}_{\mathbf{z}_0, \mathbf{z}_1, t \sim \mathcal{U}(0,1)} \|\mathbf{v}_t - \mathbf{v}_\theta(\mathbf{z}_t, \mathbf{z}_s, y, t)\|_2^2, \quad (1)$$

where  $\mathbf{z}_s$  is the latent representation of the start frame,  $y$  is the corresponding text prompt for the I2V generation task.

### 2.2. Temporal Fidelity Modulation Reference

The VFI task generates  $N'$  intermediate frames  $\mathbf{x} = \{\mathbf{I}^n\}_{n=1}^{N'}$  between the start frame  $\mathbf{I}_s$  and end frame  $\mathbf{I}_e$ . We propose a temporal reference strategy by concatenating the latents of boundary frames  $\mathbf{z}_s = \mathcal{E}(\mathbf{I}_s)$ ,  $\mathbf{z}_e = \mathcal{E}(\mathbf{I}_e)$ , and noisy intermediate latents  $\{\mathbf{z}^n\}_{n=1}^N$  along the temporal dimension, forming  $\mathcal{Z} = \{\mathbf{z}_s, \mathbf{z}^n, \mathbf{z}_e\}$ . Intermediate frames are generated by denoising  $\mathbf{z}^n$  guided by  $\mathbf{z}_s, \mathbf{z}_e$ .

In DiT [23], timestep  $t$  and text condition  $y$  jointly control modulation parameters scale, shift, and gate  $(\gamma, \beta, \alpha)$ , with  $t$  controlling the denoising intensity: stronger at the start ( $t = 1$ ) and weaker at the end ( $t = 0$ ). However, applying uniform velocity prediction  $\mathbf{v}_\theta(\mathcal{Z}, y, t)$  to all latents in  $\mathcal{Z}$  may perturb clean boundary latents.

**Fidelity Modulation.** To preserve the integrity of the boundary frames, we assign a fixed timestep  $t^* = 0$  for  $\mathbf{z}_s$  and  $\mathbf{z}_e$ , corresponding to the noise-free state, while intermediate frames retain the standard schedule. Then, the predicted velocity is:

$$\mathbf{v}_\theta(\mathcal{Z}(t^*), y, t) = \mathbf{v}_\theta(\{\mathbf{z}_s(t^*), \mathbf{z}_t^n, \mathbf{z}_e(t^*)\}, y, t). \quad (2)$$

This preserves boundary fidelity and constrains intermediate motion. Thus, the flow matching loss is redefined over intermediate frames:

$$\mathcal{L}_{flow} = \mathbb{E}_{\mathbf{z}_0^n, \mathbf{z}_1^n, t} \sum_{n=1}^N \|\mathbf{v}_t^n - \mathbf{v}_\theta(\mathcal{Z}(t^*), y, t)\|_2^2. \quad (3)$$

### 2.3. Temporal Difference Loss

Small motion amplitudes often yield near-static interpolations. To mitigate this, we introduce a temporal difference loss encouraging dynamic distinctions among consecutive latents:

$$\mathcal{L}_{temp} = \mathbb{E}_{\mathbf{z}_0^n, \mathbf{z}_1^n, t} \frac{1}{N-1} \sum_{n=1}^{N-1} \|(\hat{\mathbf{v}}_t^{n+1} - \hat{\mathbf{v}}_t^n) - (\mathbf{v}_t^{n+1} - \mathbf{v}_t^n)\|_2^2,$$

where  $\hat{\mathbf{v}}$  is the predicted velocity by  $\mathbf{v}_\theta$ . This alleviates the near-static behavior between adjacent frames and promotes smoother motion transitions. Consequently, the final training objective is:

$$\mathcal{L} = \mathcal{L}_{flow} + \omega \mathcal{L}_{temp}. \quad (4)$$

### 2.4. Matching Lines Condition

Maintaining structural stability under large camera motion or rapid object movement is challenging. Existing methods use dense optical flow [7] or sparse point trajectories [4] to extract semantic information, but often fail to capture accurate object structures. FCVG [5] introduces frame-wise conditions via ControlNeXt [24] architecture, while it may be incompatible with modern large-scale I2V models [22], which employ temporally compressed VAEs ( $\lambda_t > 1$ ), where a single latent frame influences multiple image frames during decoding. Thus, directly applying frame-wise features to video latent risks introducing incorrect structural information.

To overcome this, we extract semantically consistent line pairs from the start frame  $\mathbf{I}_s$  and end frame  $\mathbf{I}_e$  using GlueStick [25]. A lightweight ResNet-based line encoder encodes them into condition features  $\mathbf{c}_s$  and  $\mathbf{c}_e$ , which are fused with boundary latents through element-wise addition:  $\mathbf{z}'_s = \mathbf{z}_s + \mathbf{c}_s$ ,  $\mathbf{z}'_e = \mathbf{z}_e + \mathbf{c}_e$ . Then, the

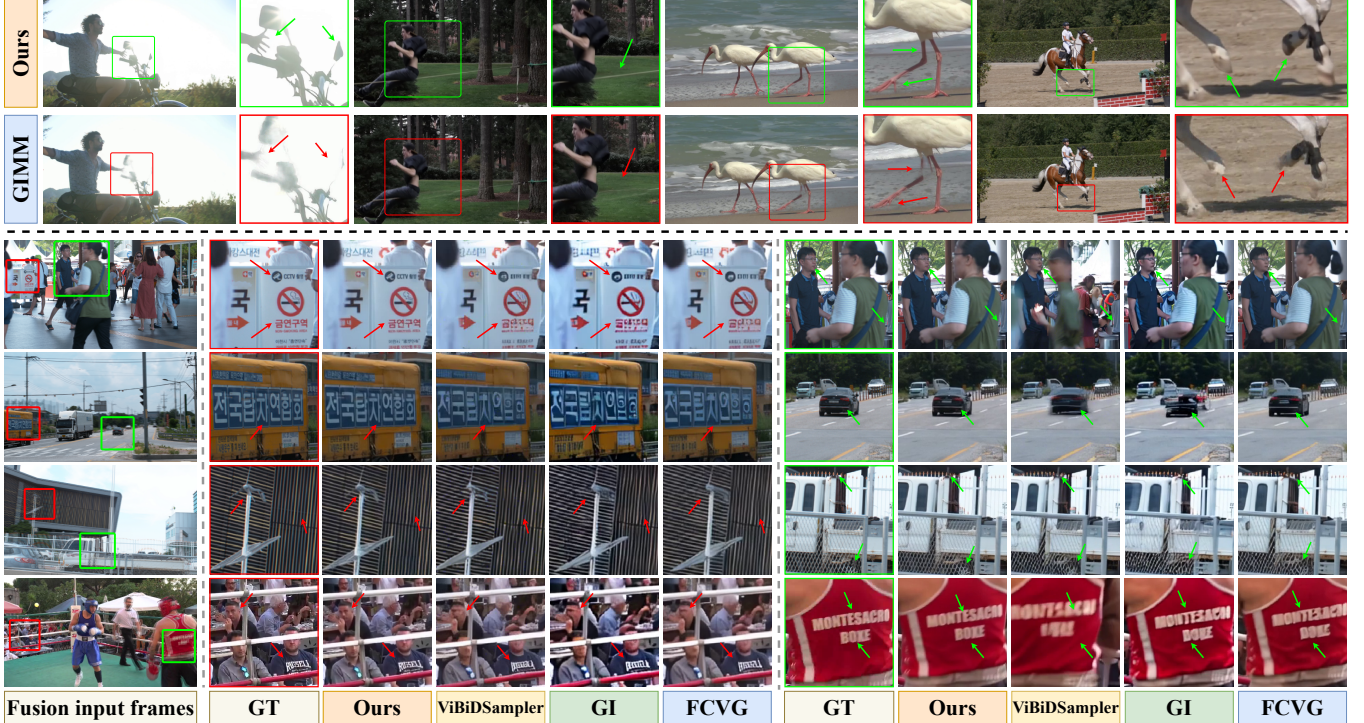


**Fig. 2. Qualitative comparison of interpolation results.** (Top) Comparison with GIMM-VFI [17] on DAVIS-2017 [18] at  $2560 \times 1440$  resolution under  $8\times$  interpolation. Ours better handles challenging conditions such as high-contrast lighting, small objects, and occlusion, avoiding artifacts like ghosting and structural distortion. (Bottom) Comparison with diffusion-based methods (GI [12], ViBiDSampler [11], FCVG [5]) on X-Test [19] and DAVIS-2017 at  $1024 \times 576$  resolution under  $8\times$  interpolation. FC-VFI preserves finer details (e.g., text, license plates, building textures), while other methods suffer from motion ambiguity and temporal artifacts.

updated sequence  $\mathcal{Z}' = \{\mathbf{z}'_s, \mathbf{z}'^n, \mathbf{z}'_e\}$  is processed by a single replicated DiT block, yielding residual features  $\mathbf{z}'_{res}$ . After normalization, they are injected into the backbone by:

$$\mathbf{z}'_{updated} = \mathbf{z}'^n + \eta \mathbf{z}'_{res}, \quad (5)$$

where  $\eta$  controls injection strength. This strategy avoids using single-frame-scale features to control multi-frame-scale video latents, preventing structural interference and enhancing object structural stability in fast motion scenarios. We introduce only 2.7% extra parameters—significantly lighter than ControlNet [26] architecture, which duplicates a significant portion of the backbone modules.

### 3. EXPERIMENTS

#### 3.1. Experimental Setup

**Training Datasets.** We construct a diverse mixed dataset from REDS [27] and Adobe240 [28], covering a wide range of real-world scenarios captured by various devices. All videos are resized to  $1280 \times 720$  and uniformly segmented into non-overlapping 9-frame clips, resulting in 13,200 clips at 120 FPS and 13,653 clips at 240 FPS, used for training  $4\times$  and  $8\times$  interpolation, respectively.

**Evaluation Metrics.** To comprehensively evaluate our model’s VFI performance, we adopt FVD [29] for video quality and motion coherence, and use FID [30], LPIPS [31], PSNR, and SSIM [32] to evaluate the visual fidelity and perceptual quality of the interpolated frame individually, following FCVG [5] and Framer [4]. Our test dataset comprises 97 high-frame-rate videos from X-Test [19], BVI-DVC [33], and DAVIS-2017 [18], yielding 326 start-and-end frame input pairs for comprehensive evaluation.

**Implementation Details.** Our model is based on the FM-based HunyuanVideo-I2V model, fine-tuned using LoRA [34] with a rank of 64. We set the hyperparameters in Eq. 4 and Eq. 5 to  $\omega = 0.8$  and  $\eta = 1.0$ . The depth of the replicated DiT block is 1, adding only 2.7% parameters. Training is performed in two stages: (1) fine-tuning the DiT backbone with LoRA for 1 epoch, and (2) full-training the line encoder and fine-tuning image-attention-related modules in DiT blocks with LoRA for 0.5 epochs.

#### 3.2. Comparisons with SOTA Models

To evaluate the performance of our proposed FC-VFI model, we conduct a comparative analysis with SOTA video frame interpolation methods developed in the past two years, encompassing both optical-flow-based (GIMM-VFI [17]) and diffusion-based approaches (FCVG [5], ViBiDSampler [11], and GI [12]).

**Quantitative Results.** As shown in Table 1, we conduct quantitative comparisons across two resolution settings:  $2560 \times 1440$  and  $1024 \times 576$ . Under the high-resolution setting, our method achieves competitive performance compared to GIMM-VFI. In contrast, when evaluated under  $1024 \times 576$  resolution, our method clearly surpasses all recent diffusion-based approaches across all five metrics, under both  $4\times$  and  $8\times$  interpolation settings, reflecting superior reconstruction fidelity and perceptual quality.

**Qualitative Results.** As illustrated in Fig. 2 (Top), our method exhibits strong visual performance compared to GIMM-VFI. Notably, although our model is trained on  $1280 \times 720$  resolution videos, it generalizes well to high-resolution scenarios, since it employs TFMR to propagate fidelity information from the boundary frames to intermediate frames. Fig. 2 (Bottom) presents visual comparisons

Methods		4×					8×				
<b>Optical-flow-based methods</b>		PSNR ↑	SSIM ↑	FID ↓	FVD ↓	LPIPS ↓	PSNR ↑	SSIM ↑	FID ↓	FVD ↓	LPIPS ↓
GIMM-VFI [17]		29.05	0.901	16.22	125.42	0.061	29.49	0.907	14.75	192.36	0.048
Ours (2560 × 1440)		30.25	0.915	15.73	130.65	0.054	30.16	0.912	15.50	194.19	0.046
<b>Diffusion-based methods</b>		PSNR ↑	SSIM ↑	FID ↓	FVD ↓	LPIPS ↓	PSNR ↑	SSIM ↑	FID ↓	FVD ↓	LPIPS ↓
GI [12]		20.96	0.847	37.58	1310.80	0.119	21.05	0.694	39.24	940.72	0.128
ViBiDSampler [11]		23.48	0.764	31.92	1375.15	0.107	20.99	0.699	36.74	978.68	0.125
FCVG [5]		26.70	0.830	20.12	330.04	0.055	25.80	0.811	21.79	251.10	0.059
<b>Ours (1024 × 576)</b>		<b>31.09</b>	<b>0.927</b>	<b>14.15</b>	<b>120.13</b>	<b>0.042</b>	<b>31.21</b>	<b>0.917</b>	<b>14.03</b>	<b>187.10</b>	<b>0.041</b>

**Table 1.** Quantitative comparison with optical-flow-based methods (evaluated at 2560 × 1440) and diffusion-based methods (evaluated at 1024 × 576) under 4× and 8× interpolation settings.

Methods		4×					8×				
<i>Different Variants</i>		PSNR ↑	SSIM ↑	FID ↓	FVD ↓	LPIPS ↓	PSNR ↑	SSIM ↑	FID ↓	FVD ↓	LPIPS ↓
Channel Reference		26.07	0.868	68.16	293.83	0.1067	24.73	0.839	70.19	501.84	0.1359
Temporal Reference (our baseline)		29.83	0.921	24.79	185.67	0.0672	27.34	0.893	32.33	407.10	0.1021
+ Fidelity Modulation (Sec. 2.2)		30.65	0.925	<b>14.78</b>	178.82	0.0552	<u>28.69</u>	0.906	<u>20.42</u>	326.37	<b>0.0832</b>
+ $\mathcal{L}_{temp}$ (Sec. 2.3)		<u>30.75</u>	<u>0.926</u>	15.48	165.87	<b>0.0548</b>	28.67	<u>0.907</u>	<b>19.96</b>	<u>312.64</u>	0.0845
+ Matching Lines Condition (Sec. 2.4)		<b>30.89</b>	<b>0.928</b>	17.19	<b>153.34</b>	<u>0.0550</u>	<b>29.13</b>	<b>0.912</b>	21.44	<b>302.04</b>	<b>0.0832</b>

**Table 2.** Ablation study demonstrating the impact of temporal reference (baseline), fidelity modulation, temporal difference loss  $\mathcal{L}_{temp}$ , and matching lines condition on interpolation quality. A channel reference (the variant using only channel-wise concatenation) is also included for comparison. Metrics are reported for 4× and 8× settings.

Method	NFE	Time (s) (4×)	Time (s) (8×)	Resolution
GI [12]	300	606	606	1024 × 576
ViBiDSampler [11]	50	23	38	1024 × 576
FCVG [5]	50	89	145	1024 × 576
<b>Ours</b>	<b>10</b>	<b>16</b>	<b>22</b>	1024 × 576
<b>Ours</b>	<b>10</b>	27	37	<b>1280 × 720</b>

**Table 3.** Our method achieves significantly faster inference compared to other diffusion-based approaches.

with recent diffusion-based methods, FC-VFI better reconstructs fine-grained details such as billboard text, license plates, and dense architectural patterns. These results validate the advantage of our method in preserving both motion consistency and visual fidelity.

### 3.3. Computation Efficiency

Although FC-VFI is built upon the large-scale HunyuanVideo-I2V backbone with 13B parameters, it achieves efficient inference by requiring only a few denoising steps. In particular, the proposed TFMR reduces the denoising complexity at each timestep, enabling high-quality interpolation with only 10 steps. As shown in Table 3, we compare with recent diffusion-based methods (GI, ViBiDSampler, and FCVG) at 1024 × 576. These methods typically rely on multi-stage denoising process or high numbers of function evaluations (NFE). In contrast, FC-VFI achieves faster inference with significantly fewer steps, even at a higher resolution of 1280 × 720.

### 3.4. Ablation Study

We conduct ablations to assess the contribution of each component, as shown in Table 2 and Fig. 3. All experiments are performed on testset at 1280 × 720 resolution. We first compare with a naive channel reference that feeds start and end frame through channel concatenation. This strategy degrades structural consistency and visual detail (third vs. fourth row in Table 2). In contrast, the temporal reference baseline concatenates start and end frame along temporal dimension, providing clearly motion boundary.

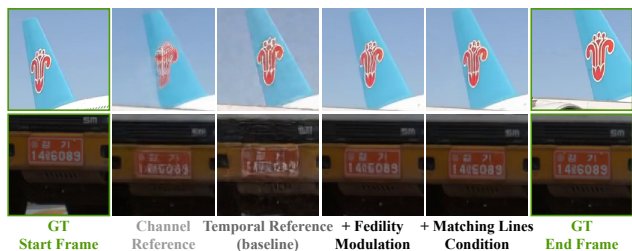


**Fig. 3.** Ablation results of our method visualized under different module configurations. The displayed intermediate frame is closer to the end frame.

Building on temporal reference, the fidelity modulation mechanism further improves structural fidelity by explicitly correcting timestep noise in boundary frame conditioning (comparing the fourth and fifth row in Table 2). Adding the temporal difference loss  $\mathcal{L}_{temp}$  leads to smoother transitions across intermediate frames, enhancing temporal coherence (fifth row v.s. sixth row in Table 2). Finally, incorporating the matching lines condition yields the most refined results by injecting line-level correspondence priors (sixth row v.s. seventh row in Table 2), improving detail restoration such as edges and textures.

## 4. CONCLUSION

In this paper, we propose FC-VFI, a diffusion-based video frame interpolation (VFI) framework finetuned from a pre-trained IV2 model (e.g., HunyuanVideo-I2V). Our framework introduces Temporal Fidelity Modulation Reference (TFMR), which propagates the fidelity information from the start and end frames using temporal concatenation and fidelity modulation, enabling efficient inference within only 10 denoising steps. In addition, we design a novel temporal difference loss and a matching-lines-based control strategy to further enhance temporal consistency and reduce artifacts. Extensive experiments on public datasets demonstrate the effectiveness of our method, particularly in high-FPS video frame interpolation.

## 5. REFERENCES

- [1] Wonyong Seo, Jihyong Oh, and Munchurl Kim, “Bim-vfi: Bidirectional motion field-guided frame interpolation for video with non-uniform motions,” in *CVPR*, 2025.
- [2] Xiaogang Xu, Yi Wang, Liwei Wang, Bei Yu, and Jiaya Jia, “Conditional temporal variational autoencoder for action video prediction,” *IJCV*, 2023.
- [3] Zhewei Huang, Tianyuan Zhang, Wen Heng, Boxin Shi, and Shuchang Zhou, “Real-time intermediate flow estimation for video frame interpolation,” in *ECCV*, 2022.
- [4] Wen Wang, Qiuyu Wang, Kecheng Zheng, Hao Ouyang, Zhekai Chen, Biao Gong, Hao Chen, Yujun Shen, and Chunhua Shen, “Framer: Interactive frame interpolation,” in *ICLR*, 2025.
- [5] Tianyi Zhu, Dongwei Ren, Qilong Wang, Xiaohe Wu, and Wangmeng Zuo, “Generative inbetweening through frame-wise conditions-driven video generation,” in *CVPR*, 2025.
- [6] Chenglu Pan, Xiaogang Xu, Ganggui Ding, Yunke Zhang, Wenbo Li, Jiarong Xu, and Qingbiao Wu, “Boosting diffusion-based text image super-resolution model towards generalized real-world scenarios,” in *ICCVW*, 2025.
- [7] Guozhen Zhang, Yuhan Zhu, Yutao Cui, Xiaotong Zhao, Kai Ma, and Limin Wang, “Motion-aware generative frame interpolation,” *arXiv preprint arXiv:2501.03699*, 2025.
- [8] Duolikun Danier, Fan Zhang, and David Bull, “Ldmvfi: Video frame interpolation with latent diffusion models,” in *AAAI*, 2024.
- [9] Xiaogang Xu, Hengshuang Zhao, Vibhav Vineet, Ser-Nam Lim, and Antonio Torralba, “Mtfomer: Multi-task learning via transformer and cross-task reasoning,” in *ECCV*, 2022.
- [10] Haiwen Feng, Zheng Ding, Zhihao Xia, Simon Niklaus, Victoria Abrevaya, Michael J Black, and Xuaner Zhang, “Explorative inbetweening of time and space,” in *ECCV*, 2024.
- [11] Serin Yang, Taesung Kwon, and Jong Chul Ye, “Vibidsampler: Enhancing video interpolation using bidirectional diffusion sampler,” in *ICLR*, 2025.
- [12] Xiaojuan Wang, Boyang Zhou, Brian Curless, Ira Kemelmacher-Shlizerman, Aleksander Holynski, and Steven M Seitz, “Generative inbetweening: Adapting image-to-video models for keyframe interpolation,” in *ICLR*, 2025.
- [13] Zhen Yang, Ganggui Ding, Wen Wang, Hao Chen, Bohan Zhuang, and Chunhua Shen, “Object-aware inversion and re-assembly for image editing,” *arXiv preprint arXiv:2310.12149*, 2023.
- [14] Andreas Blattmann, Tim Dockhorn, Sumith Kulal, Adam Letts, et al., “Stable video diffusion: Scaling latent video diffusion models to large datasets,” *arXiv*, 2023.
- [15] Ganggui Ding, Canyu Zhao, Wen Wang, Zhen Yang, Zide Liu, Hao Chen, and Chunhua Shen, “Freecustom: Tuning-free customized image generation for multi-concept composition,” in *CVPR*, 2024.
- [16] Xiaogang Xu and Ning Xu, “Hierarchical image generation via transformer-based sequential patch selection,” in *AAAI*, 2022.
- [17] Zujin Guo, Wei Li, and Chen Change Loy, “Generalizable implicit motion modeling for video frame interpolation,” *NeurIPS*, 2024.
- [18] Jordi Pont-Tuset, Federico Perazzi, Sergi Caelles, Pablo Arbeláez, Alex Sorkine-Hornung, and Luc Van Gool, “The 2017 davis challenge on video object segmentation,” *arXiv preprint arXiv:1704.00675*, 2017.
- [19] Hyeonjun Sim, Jihyong Oh, and Munchurl Kim, “Xvfi: extreme video frame interpolation,” in *ICCV*, 2021.
- [20] Yaron Lipman, Ricky TQ Chen, Heli Ben-Hamu, Maximilian Nickel, and Matt Le, “Flow matching for generative modeling,” *arXiv preprint arXiv:2210.02747*, 2022.
- [21] Diederik P Kingma and Max Welling, “Auto-encoding variational bayes,” *arXiv preprint arXiv:1312.6114*, 2013.
- [22] Weijie Kong, Qi Tian, Zijian Zhang, Rox Min, Zuozhuo Dai, Jin Zhou, Jiangfeng Xiong, Xin Li, Bo Wu, Jianwei Zhang, et al., “Hunyuanvideo: A systematic framework for large video generative models,” *arXiv*, 2024.
- [23] William Peebles and Saining Xie, “Scalable diffusion models with transformers,” in *ICCV*, 2023.
- [24] Bohao Peng, Jian Wang, Yuechen Zhang, Wenbo Li, Ming-Chang Yang, and Jiaya Jia, “Controlnext: Powerful and efficient control for image and video generation,” *arXiv preprint arXiv:2408.06070*, 2024.
- [25] Rémi Patrat, Iago Suárez, Yifan Yu, Marc Pollefeys, and Viktor Larsson, “Gluestick: Robust image matching by sticking points and lines together,” in *CVPR*, 2023.
- [26] Lvmin Zhang, Anyi Rao, and Maneesh Agrawala, “Adding conditional control to text-to-image diffusion models,” in *ICCV*, 2023.
- [27] Seungjun Nah, Sungyong Baik, Seokil Hong, Gyeongsik Moon, Sanghyun Son, Radu Timofte, and Kyoung Mu Lee, “Ntire 2019 challenge on video deblurring and super-resolution: Dataset and study,” in *CVPRW*, 2019.
- [28] Wang Shen, Wenbo Bao, Guangtao Zhai, Li Chen, Xiongkuo Min, and Zhiyong Gao, “Blurry video frame interpolation,” in *CVPR*, 2020.
- [29] Thomas Unterthiner, Sjoerd Van Steenkiste, Karol Kurach, Raphael Marinier, Marcin Michalski, and Sylvain Gelly, “Towards accurate generative models of video: A new metric & challenges,” *arXiv*, 2018.
- [30] Martin Heusel, Hubert Ramsauer, Thomas Unterthiner, Bernhard Nessler, and Sepp Hochreiter, “Gans trained by a two time-scale update rule converge to a local nash equilibrium,” *Advances in neural information processing systems*, 2017.
- [31] Richard Zhang, Phillip Isola, Alexei A Efros, Eli Shechtman, and Oliver Wang, “The unreasonable effectiveness of deep features as a perceptual metric,” in *CVPR*, 2018.
- [32] Zhou Wang, Alan C Bovik, Hamid R Sheikh, and Eero P Simoncelli, “Image quality assessment: from error visibility to structural similarity,” *IEEE transactions on image processing*, vol. 13, no. 4, pp. 600–612, 2004.
- [33] Di Ma, Fan Zhang, and David R Bull, “Bvi-dvc: A training database for deep video compression,” *IEEE Transactions on Multimedia*, 2021.
- [34] Edward J Hu, Yelong Shen, Phillip Wallis, Zeyuan Allen-Zhu, Yuanzhi Li, Shean Wang, Lu Wang, Weizhu Chen, et al., “Lora: Low-rank adaptation of large language models,” in *ICLR*, 2022.

- [35] Jingxi Chen, Brandon Y Feng, Haoming Cai, Tianfu Wang, Levi Burner, Dehao Yuan, Cornelia Fermuller, Christopher A Metzler, and Yiannis Aloimonos, “Repurposing pre-trained video diffusion models for event-based video interpolation,” in *CVPR*, 2025.
- [36] Team Wan, Ang Wang, Baole Ai, Bin Wen, Chaojie Mao, Chen-Wei Xie, Di Chen, Feiwu Yu, Haiming Zhao, Jianxiao Yang, Jianyuan Zeng, Jiayu Wang, Jingfeng Zhang, Jingren Zhou, Jinkai Wang, Jixuan Chen, Kai Zhu, Kang Zhao, Keyu Yan, Lianghua Huang, Mengyang Feng, Ningyi Zhang, Pandeng Li, Pingyu Wu, Ruihang Chu, Ruili Feng, Shiwei Zhang, Siyang Sun, Tao Fang, Tianxing Wang, Tianyi Gui, Tingyu Weng, Tong Shen, Wei Lin, Wei Wang, Wei Wang, Wenmeng Zhou, Wente Wang, Wenting Shen, Wenyuan Yu, Xianzhong Shi, Xiaoming Huang, Xin Xu, Yan Kou, Yangyu Lv, Yifei Li, Yijing Liu, Yiming Wang, Yingya Zhang, Yitong Huang, Yong Li, You Wu, Yu Liu, Yulin Pan, Yun Zheng, Yuntao Hong, Yupeng Shi, Yutong Feng, Zeyinzi Jiang, Zhen Han, Zhi-Fan Wu, and Ziyu Liu, “Wan: Open and advanced large-scale video generative models,” *arXiv*, 2025.
- [37] Zhuoyi Yang, Jiayan Teng, Wendi Zheng, Ming Ding, Shiyu Huang, Jiazheng Xu, Yuanming Yang, Wenyi Hong, Xiaohan Zhang, Guanyu Feng, et al., “Cogvideox: Text-to-video diffusion models with an expert transformer,” in *ICLR*, 2025.

## A. SUPPLEMENTARY MATERIALS

### A.1. Additional Qualitative Results

To further demonstrate the robust stability and structural consistency of our proposed FC-VFI, we provide additional qualitative comparisons with state-of-the-art methods in Figure 4. Following the identical evaluation setting as the main text, we compare our method against the representative optical-flow-based method GIMM-VFI [17] at high resolution ( $2560 \times 1440$ ), and recent diffusion-based methods (GI [12], ViBiDSampler [11], and FCVG [5]) at  $1024 \times 576$  resolution.

As illustrated in the newly added diverse test scenes, FC-VFI consistently preserves fine-grained details and structural integrity, even in highly challenging scenarios involving complex textures, extreme object motions, and severe occlusions. In contrast, the baseline approaches still suffer from noticeable visual degradation, including structural distortion, motion ambiguity, and ghosting artifacts. These supplementary visual results further validate the generalizability and superiority of our Temporal Fidelity Modulation Reference (TFMR) and matching-lines condition mechanisms.

### A.2. Paradigm Comparison with Diffusion Based Methods.

Previous diffusion-based video frame interpolation methods can be categorized into Time Reversal and Channel Reference paradigms, as depicted in Fig. 5.

**Time Reversal methods**, including TRF [10], GI [12], ViBiDSampler [11], RE-VDM [35], and FCVG [5], rely on conditional diffusion models, performing two image-to-video (I2V) generations conditioned on the start ( $\mathbf{z}_s$ ) and end ( $\mathbf{z}_e$ ) frames, respectively, followed by a fusion mechanism. These methods typically require two denoising passes, significantly increasing computational complexity. Some incorporate re-noising (TRF [10], GI [12]) to smooth intermediate frames, further elevating the number of function evaluations (NFE) and causing instability, particularly motion reversal artifacts in scenes with fast-moving objects or complex camera dynamics, compromising structural integrity and motion continuity.

**Channel Reference methods** integrate boundary frame information via channel concatenation or element-wise feature addition, as seen in Framer [4]. These methods require the base I2V model to support channel-wise conditioning, limiting compatibility with models like HunyuanVideo-I2V [22], which use alternative conditioning mechanisms. Adapting HunyuanVideo-I2V for channel reference necessitates training a new Patch Embedder, disrupting the pre-trained prior of its large-scale DiT backbone and degrading interpolation quality, such as visual fidelity and structural integrity. This constraint restricts deployment flexibility for such methods.

Our proposed **Temporal Reference paradigm** concatenates boundary frames  $\mathbf{z}_s, \mathbf{z}_e$  in the temporal dimension, providing explicit, high-fidelity reference conditions for the noise latent, aligning with video temporal modeling. This temporal concatenation seamlessly integrates with the token-wise input mechanism of modern DiT-based models, enhancing the denoising process’s initialization. The Temporal Fidelity Modulation Reference (TFMR) mechanism enhances motion trajectory and detail capture via modulated boundary frame information, enabling robust high-resolution interpolation (e.g.,  $2560 \times 1440$ ) with reduced motion blur and structural distortion in challenging scenarios like occlusions or weak textures. Compatible with diverse architectures, including HunyuanVideo-I2V [22], WAN [36], and SVD [14], FC-VFI with TFMR offers a versatile, high-performance solution for video frame interpolation, achieving superior quality and generalization.

### A.3. High Resolution Frames Interpolation.

Our Temporal Fidelity Modulation Reference (TFMR) mechanism enables high-fidelity interpolation of intermediate frames by leveraging modulated boundary frame information. Despite pre-training and fine-tuning the base FC-VFI model on datasets with a maximum resolution of  $1280 \times 720$ , our approach generalizes robustly to  $2560 \times 1440$ , achieving high-quality zero-shot interpolation. Fig. 6 presents qualitative results on the X-Test dataset [19] at  $2560 \times 1440$ , demonstrating FC-VFI’s superior performance in challenging scenarios, including text, dense textures, buildings, faces, and license plates. Compared to ground-truth, our method preserves structural integrity and visual fidelity, showcasing its effectiveness in high-resolution video frame interpolation.

### A.4. Limitations and Future Work.

**Limitations.** Although FC-VFI achieves lower inference times than existing diffusion-based methods, its Temporal Reference mechanism, which leverages boundary frames  $\mathbf{z}_s, \mathbf{z}_e$  to enhance intermediate frame quality, introduces additional computational overhead in the temporal dimension. The Matching-Lines Condition, limited by the video latent’s multi-frame decoding nature, cannot explicitly control intermediate frames  $\{\mathbf{z}^n\}$  like FCVG [5]. Instead, it enhances boundary frames’ semantic information

$$\mathbf{z}'_s = \mathbf{z}_s + \mathbf{c}_s, \mathbf{z}'_e = \mathbf{z}_e + \mathbf{c}_e$$

to indirectly improve DiT’s feature capture, constraining control flexibility. Currently, FC-VFI is validated only on HunyuanVideo-I2V, lacking evaluation on other models like CogVideoX [37] or WAN [36]. Performance in complex dynamic scenes (e.g., water, smoke) is limited by training data and base model capabilities.

**Future Work.** We aim to enhance inference efficiency by reducing the current 10-step inference to 5 steps or single-step via model distillation and attention parallelization, narrowing the efficiency gap with optical flow methods at high resolutions (e.g.,  $2560 \times 1440$ ). We plan to validate the Temporal Fidelity Modulation Reference (TFMR) framework on diverse architectures like WAN [36], exploring its generalization. Additionally, extending training data and model capacity will enable 4K resolution and high-rate interpolation ( $16 \times$  or  $32 \times$ ) for higher-fidelity VFI.

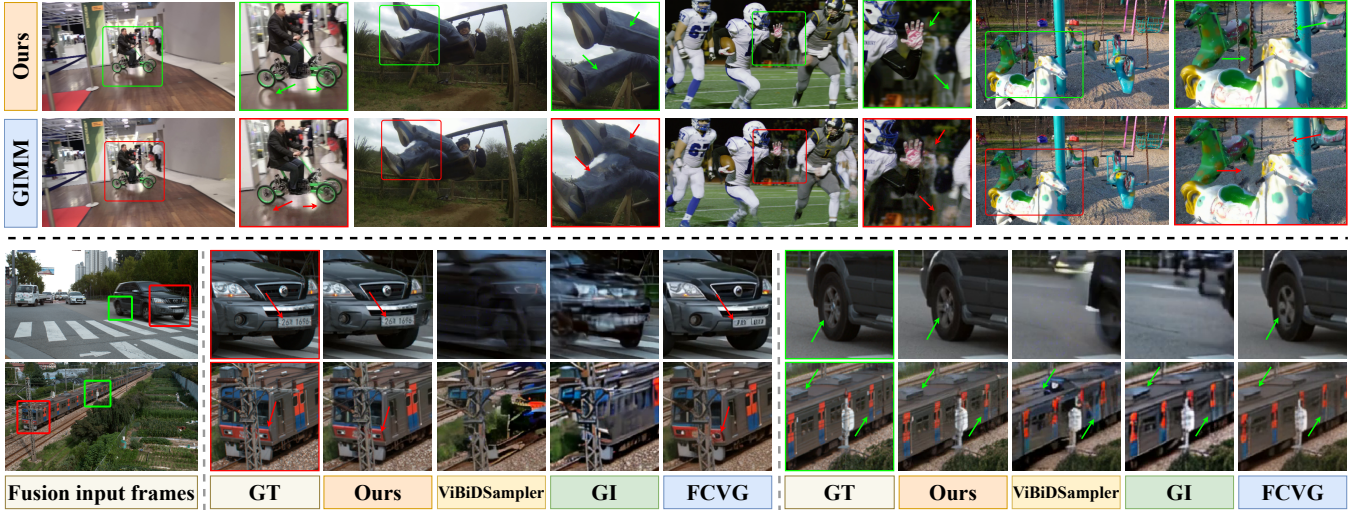


**Fig. 4.** Additional qualitative comparison of interpolation results. (Top) Visual comparisons with GIMM-VFI [17] at  $2560 \times 1440$  resolution under  $8 \times$  interpolation. Tested on additional challenging scenes, our FC-VFI effectively suppresses structural distortion and ghosting artifacts. (Bottom) Visual comparisons with recent diffusion-based methods (GI [12], ViBiDSampler [11], and FCVG [5]) at  $1024 \times 576$  resolution under  $8 \times$  interpolation. FC-VFI consistently demonstrates superior capability in recovering fine details (e.g., complex boundaries and textual patterns) and maintaining temporal consistency compared to the baselines (Sec. A.1).

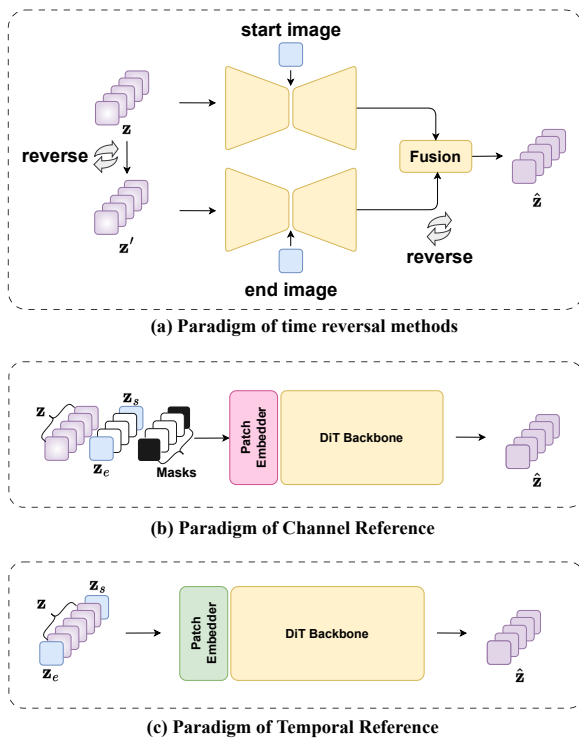


**Fig. 5.** Comparison of Time Reversal, Channel Reference, and Temporal Reference paradigms for diffusion-based video frame interpolation (Sec. A.2).

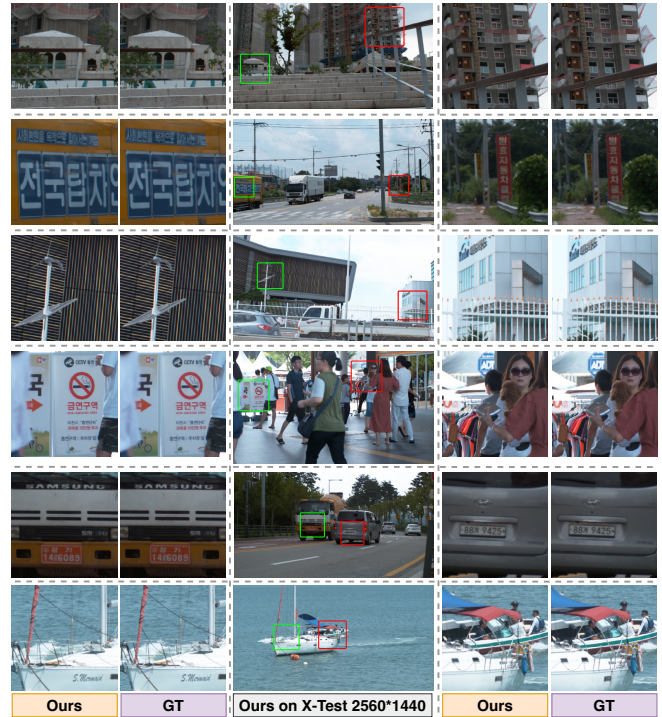


**Fig. 6.** Qualitative results of FC-VFI on the X-Test dataset [19] at  $2560 \times 1440$  (zero-shot). The center shows a thumbnail of the interpolated frame (non-native resolution), with the left panel comparing our result (green box) to ground-truth and the right panel comparing our result (red box) to ground-truth (Sec. A.3).